

# Adjoint-based Accelerated Adaptive Refinement in Frequency Domain 3-D Finite Element Method Scattering Problems

Jake J. Harmon, *Student Member, IEEE*, Cam Key, *Student Member, IEEE*, Don Estep, Troy Butler, and Branislav M. Notaroš, *Fellow, IEEE*

**Abstract**—We present the application of adjoint analysis to 3-D finite element method scattering problems for a posteriori error estimation and adaptive refinement. Adjoint-based methodologies, though underutilized in computational electromagnetics (CEM), enable significant improvements for both efficiency and accuracy. We first formulate the adjoint problem of the 3-D double-curl wave equation and the error estimates for the construction of novel accelerated adaptive refinement algorithms. We demonstrate adaptive error control for a customizable quantity of interest (QoI) resulting in targeted refinement and improved resource allocation through application of automatic global and local error tolerance heuristics which accelerate the refinement process. The proposed refinement algorithms rapidly refine even extremely coarse initial discretizations to high accuracy, eliminating or substantially reducing manual intervention in the generation of computationally efficient and accurate simulations. Moreover, comparisons with analytical results validate our approach to accelerating automatic refinement to fine tolerances.

**Index Terms**—A posteriori error analysis, adaptive error control, adaptive mesh refinement, adjoint methods, computational electromagnetics, error estimation, finite element method, frequency domain.

## I. INTRODUCTION

THE adjoint solution, a generalized Green's function, though underutilized in computational electromagnetics (CEM), offers a wealth of opportunity and advantages for the development and testing of efficient, accurate, and practical applications. Analyzing the traditional problem along with its adjoint (or dual) enables a fundamental revision of the connection between the quality and outcome of a solution and the underlying discretization on which it is founded, as well as the physical parameters of the problem (e.g., the conductivity or permittivity).

The selection of regions of a discretization for refinement has traditionally relied on various heuristics. Typical heuris-

tics rely on classifying the smoothness of the solution in some norm, or standard residual estimates [1], [2]. Unknowns are added (or redistributed) according to the chosen criteria through some adaptive algorithm.

However, these standard approaches often grossly overestimate error with excessively large bounds or may fail to control the error [3]. In most applications the solution itself is not the desired computable, but rather some functional of the solution computed by post-processing: the radar cross section (RCS) or S-parameters, for instance. Application of the adjoint problem addresses this drawback. The dual weighted residual (DWR) expression of the error in a desired quantity of interest (QoI) permits a detailed inspection of the impact of the discretization on the error [2]–[5]. By weighting the error residual by the coefficients from the adjoint solution, the stability properties of the problem are included, improving the correspondence between refinement choices and the accuracy of the QoI.

Reducing or eliminating the need for expert user intervention in the creation and refinement of discretizations for accurate and efficient modeling in CEM provides significant value for resource and time savings. For iterative design or optimization procedures, an adjoint informed approach yields highly targeted information, permitting the tailoring of the discretization for accuracy and cost minimization by simultaneously categorizing insufficient and inefficient regions of a discretization.

In applied mathematics and other computational fields such as computational fluid dynamics, adjoint analysis has benefited from extensive research. For a comprehensive theory of adjoint-based error estimation see [2], [6], [7]. For additional background and applications to specific partial differential equations, see [3], [8]–[12].

In CEM, on the other hand, adjoint analysis has largely focused on estimation of gradients and sensitivity analysis built for optimization in finite-difference time-domain methods, as in [13]–[21], rather than the error estimation and adaptive refinement for frequency domain methods of this work.

Previous work in CEM regarding a *posteriori* error estimation and adaptive refinement as in [22], [23], based on the element residual method (ERM), and the estimator in [24] both demonstrate reliable error indicators. However, such refinement strategies do not involve a targeted QoI or post-processing of the numerical solution presented in this work, nor the focus on expediting the refinement process. Notably in [25], [26], a *posteriori* error bounds derived by duality

Manuscript received February 21, 2020; revised May 27, 2020; accepted July 3, 2020. This work was supported by the US Air Force Research Laboratory, CREATE SENTRI, Riverside Research Institute, under contract FA8650-14-D-1725(6F1957).

Jake J. Harmon, Cam Key, and Branislav M. Notaroš are with the department of Electrical and Computer Engineering, Colorado State University, Fort Collins, CO 80523-1373 USA (e-mail: j.harmon@colostate.edu, branislav.notaros@colostate.edu, camkey@rams.colostate.edu).

Donald Estep is with the Department of Statistics, Colorado State University, Fort Collins, CO, USA (e-mail: donald.estep@colostate.edu).

Troy Butler is with the Department of Mathematical and Statistical Sciences, University of Colorado Denver, Denver, CO, USA (email: troy.butler@ucdenver.edu).

arguments show adaptive refinement capability, though only for a specific far-field pattern QoI and with severe limitations both in the geometric discretization and the field expansion. This work, in contrast, applies to arbitrary geometries, low- and high-order finite elements, and applies to arbitrary QoIs through substitution of additional adjoint excitations, while also emphasizing the acceleration of the refinement procedure.

Early advancements in goal-oriented adaptivity for CEM, such as in [27], [28], prioritized geometric refinement for 2-D waveguide problems and computation of  $S$ -parameters. For parallel wire and parallel plate problems, similar duality arguments to those applied in this paper were used to estimate the error in electrostatic force and capacitance quantities [29]. However, the formulation provided in [29] does not permit anisotropy in the domain, while our approach supports full anisotropy. Furthermore, instead of pure error estimation, we leverage the dual problem and novel adaptivity procedures to accelerate automatic refinement of poor quality discretizations.

Additional existing research in adaptive refinement research for CEM has largely focused on minimizing projection-based interpolation error for 1-D and 2-D problems. These methods apply both energy-norm and goal-oriented refinement to iteratively increase the resolution of a starting discretization. For energy-norm based adaptivity, such as in [30], [31], elements within an arbitrary percentage of the maximum estimated element error are refined incrementally until a convergence condition is met between successive iterations. Similar explorations in the analysis of 2-D and 3-D waveguide problems, which apply this approach of comparing coarse and fine grids (both geometrically and in field expansion) for energy-norm refinement, achieve high accuracy from poor starting discretizations [32], [33]. However, in contrast to the novel adaptivity proposed in this paper, these methods are limited to fixed resolution increases which require large iteration numbers to satisfy convergence conditions for high accuracy. Additionally, the projection-based interpolation approach permits only the adoption of finer resolution from coarse resolution, whereas our approach enables both increases and decreases in resolution, providing greater independence from the starting discretization. Moreover, existing goal-oriented refinement based on this methodology, while utilizing duality arguments as in this paper, perform adaptivity as an extension of the energy-based approach, such as for improving the analysis of  $S$ -parameters [34], [35], 2-D scattering from infinitely long cylinders and mutual coupling between antennas [36], or resistivity logging instruments [37], and as a result share the same difficulties, such as refining to high accuracy in lower iteration numbers. Notably, the paper [38] demonstrated goal-orientated refinement for analyzing scattering in cavity problems, though with limitations to circular boundaries due to its use of infinite elements for boundary truncation and with *a priori* field expansion orders.

Recent explorations in 1-D dielectric slab problems [39], along with further developments in adjoint-based error estimation [40]–[43] on which this work is based have shown further potential for adjoint-based methodologies in CEM.

The adaptivity we propose shares the advantages provided by goal-oriented refinement and duality-based error estimation

as in existing works in CEM and applied mathematics. Our approach, however, emphasizes the acceleration of the refinement procedure to enhance the practicality and efficiency of goal-oriented refinement and reduces the dependence of the number of iterations required in refinement on the desired accuracy for refinement to high accuracy in few iterations.

This paper develops a comprehensive foundation for the practical and effective application of adjoint methods to adaptive refinement in frequency domain CEM, generalizing and expanding the work introduced in [40]–[43]. We provide derivations for the adjoint problem for the 3D double-curl wave equation and the adjoint-based error estimates. In addition, we contribute novel refinement heuristics which leverage the adjoint error contribution estimates—based on the global error tolerance, and a combined *a priori-a posteriori* local error contribution estimator—for efficient, practical, and readily applicable fully-automatic refinement work which substantially and intrinsically accelerates the refinement process while maintaining efficiency with respect to desired error contribution tolerances, including for extremely coarse initial discretizations.

The rest of this paper is organized as follows. Section II describes the theory and derivations for applying the adjoint methodology to CEM, including derivations for the adjoint problem and its solution; error estimates based on the DWR; construction of completely automatic refinement heuristics which leverage the DWR estimates; and, lastly, an explicit formulation of a customizable far-field QoI. Section III provides numerical examples, illustrating the DWR error estimates and applying them to the global and local tolerance refinement heuristics using the double higher-order finite element method. The examples demonstrate rapid refinement even for extremely coarse initial discretizations with relative independence of the tolerance and number of iterations required.

## II. THE ADJOINT: DERIVATIONS AND ESTIMATORS

### A. The Adjoint Problem

We first summarize the components of the standard forward problem. In this case the governing equation for the forward problem is the double-curl wave equation:

$$\nabla \times \mu_r^{-1} \nabla \times \mathbf{E} - k_0^2 \varepsilon_r \mathbf{E} = 0, \quad (1)$$

with  $\mu_r$  and  $\varepsilon_r$  signifying the relative permeability and permittivity—which in general can be tensors—respectively, and  $k_0$  denoting the free space wave number. Separating the excitation ( $\mathbf{E}^{inc}$ ) from the response ( $\mathbf{E}^{sc}$ ), we have that

$$\nabla \times \mu_r^{-1} \nabla \times \mathbf{E}^{sc} - k_0^2 \varepsilon_r \mathbf{E}^{sc} = -\nabla \times \mu_r^{-1} \nabla \times \mathbf{E}^{inc} + k_0^2 \varepsilon_r \mathbf{E}^{inc}, \quad (2)$$

which we denote in linear operator form as

$$\mathcal{L}\mathbf{E}^{sc} = \mathbf{G}. \quad (3)$$

The domain is truncated by an air layer and a perfectly matched layer (PML). The PML is a stretched-coordinate type conformal PML which exhibits improved accuracy and improved efficiency over standard PML implementations [44].

The entire domain is then surrounded by perfect electrical conductor (PEC) which provides the Dirichlet boundary condition

$$\mathbf{n} \times \mathbf{E} = 0 \quad (4)$$

at the PEC boundary.

The adjoint operator  $\mathcal{L}^*$  is defined by the Lagrange identity [7]:

$$\langle \mathcal{L}\mathbf{u}, \mathbf{v} \rangle = \langle \mathbf{u}, \mathcal{L}^*\mathbf{v} \rangle, \quad (5)$$

with the relevant inner-product being the  $L^2$  inner-product:

$$\langle \mathbf{u}, \mathbf{v} \rangle = \int_{\Omega} \mathbf{v}^H \mathbf{u} \, d\Omega = \int_{\Omega} \mathbf{v}^* \cdot \mathbf{u} \, d\Omega, \quad (6)$$

where  $\Omega$  denotes the volume of interest.

For simplicity, we write  $\mathcal{L} = \mathcal{L}_1 - \mathcal{L}_2$ , where the operators  $\mathcal{L}_1$  and  $\mathcal{L}_2$  are clear from the derivations shown below. By the multi-linearity of the inner-product,

$$\langle \mathcal{L}\mathbf{E}^{sc}, \mathbf{v} \rangle = \langle \mathcal{L}_1\mathbf{E}^{sc}, \mathbf{v} \rangle - \langle \mathcal{L}_2\mathbf{E}^{sc}, \mathbf{v} \rangle. \quad (7)$$

Taking the first term, using standard vector calculus identities and the divergence theorem, using we have that

$$\begin{aligned} \langle \mathcal{L}_1\mathbf{E}^{sc}, \mathbf{v} \rangle &= \iiint_{\Omega} \mathbf{v}^* \cdot (\nabla \times \mu_r^{-1} \nabla \times \mathbf{E}^{sc}) \, d\Omega \\ &= \iint_S (\mu_r^{-1} \nabla \times \mathbf{E}^{sc} \times \mathbf{v}^*) \cdot d\mathbf{S} \\ &\quad + \iiint_{\Omega} \mu_r^{-1} \nabla \times \mathbf{E}^{sc} \cdot (\nabla \times \mathbf{v}^*) \, d\Omega. \end{aligned} \quad (8)$$

However, since

$$\iint_S (\mu_r^{-1} \nabla \times \mathbf{E}^{sc} \times \mathbf{v}^*) \cdot d\mathbf{S} = \iint_S (\mathbf{n} \times \mu_r^{-1} \nabla \times \mathbf{E}^{sc}) \cdot \mathbf{v}^* \, dS, \quad (9)$$

where  $d\mathbf{S} = \mathbf{n}dS$ , by (4), the surface integral term in (8) is zero. Corresponding to (4), we also have the adjoint boundary condition

$$\mathbf{n} \times \mathbf{v}^* = 0. \quad (10)$$

Repeating the procedure above implies

$$\begin{aligned} &\iiint_{\Omega} \mu_r^{-1} \nabla \times \mathbf{E}^{sc} \cdot (\nabla \times \mathbf{v}^*) \, d\Omega \\ &= \iint_S (\mathbf{E}^{sc} \times \mu_r^{-1} \nabla \times \mathbf{v}^*) \cdot d\mathbf{S} \\ &\quad + \iiint_{\Omega} \mathbf{E}^{sc} \cdot (\nabla \times \mu_r^{-1} \nabla \times \mathbf{v}^*) \, d\Omega, \end{aligned} \quad (11)$$

where the surface integral term reduces to zero analogously to (8) by the adjoint boundary condition (10).

Hence,

$$\langle \mathcal{L}_1\mathbf{E}^{sc}, \mathbf{v} \rangle = \iiint_{\Omega} \mathbf{E}^{sc} \cdot (\nabla \times \mu_r^{-1} \nabla \times \mathbf{v}^*) \, d\Omega. \quad (12)$$

Then, for the second term in (7),

$$\begin{aligned} \langle \mathcal{L}_2\mathbf{E}^{sc}, \mathbf{v} \rangle &= \iiint_{\Omega} \mathbf{v}^* \cdot (k_0^2 \varepsilon_r \mathbf{E}^{sc}) \, d\Omega \\ &= \iiint_{\Omega} \mathbf{E}^{sc} \cdot (k_0^2 \varepsilon_r \mathbf{v}^*) \, d\Omega \end{aligned} \quad (13)$$

Finally, by combining (12) and (13) as in (7), we find that the adjoint operator satisfies

$$\mathcal{L}^*\mathbf{v} = \nabla \times (\mu_r^{-1})^* \nabla \times \mathbf{v} - k_0^2 \varepsilon_r^* \mathbf{v}. \quad (14)$$

The adjoint operator therefore has the form of the forward operator, with the complex conjugate of the model parameters. (14) generalizes to tensor materials by exchanging the complex conjugate for the conjugate transpose.

Note that due to the linearity of the forward operator, the adjoint problem can be solved independently; this is not the case for non-linear operators [7].

All that remains is to choose a suitable adjoint problem which corresponds to the desired QoI. We have, for example, a collection of functionals which we desire to compute from the solution to the forward problem. In this paper we concern ourselves with examining scattered electric field quantities, though the procedure extends naturally to other QoIs.

In general, we have that for some functional  $J$  and forward solution  $\mathbf{E}^{sc}$  of  $\mathcal{L}\mathbf{E}^{sc} = \mathbf{G}$ ,

$$J[\mathbf{E}^{sc}] = QoI, \quad (15)$$

with  $J$  restricted to the set of linear functionals of  $\mathbf{E}^{sc}$ . For non-linear  $J$ , a linearized form can be substituted in (15).

By the Riesz representation theorem [51], there exists  $\mathbf{p}$  such that for all  $\mathbf{E}^{sc}$

$$J[\mathbf{E}^{sc}] = \langle \mathbf{E}^{sc}, \mathbf{p} \rangle, \quad (16)$$

which determines our choice for the adjoint excitation:

$$\mathcal{L}^*\mathbf{v} = \mathbf{p}. \quad (17)$$

Constructing the adjoint solution for any number of QoIs simply requires solving the problem with new right-hand sides corresponding to new adjoint data.

Note, however, constructing the excitation for the Galerkin solution of the adjoint problem—rather than requiring an explicit separation of  $\mathbf{p}$  from the QoI expression—entails evaluating the functional  $J$  for each component of the basis of the approximate solution. Hence, for the adjoint problem we must simply find  $\mathbf{v} \in B$  such that

$$\langle \mathcal{L}^*\mathbf{v}, \mathbf{y} \rangle = \langle \mathbf{p}, \mathbf{y} \rangle = \overline{J[\mathbf{y}]} \quad \forall \mathbf{y} \in B, \quad (18)$$

where  $\overline{J[\mathbf{y}]}$  denotes the complex conjugate of  $J[\mathbf{y}]$ .

### B. Error Estimation and Adaptive Refinement

We demonstrate how to produce an error estimate in the form of the DWR. We denote the error by

$$\mathbf{e} = \mathbf{E}^{sc} - \pi_h \mathbf{E}^{sc}, \quad (19)$$

where  $\mathbf{E}^{sc} \in B$  represents the “true” solution, and  $\pi_h \mathbf{E}^{sc} \in \pi_h B$  the Galerkin approximate solution, with  $B$  and  $\pi_h B$  denoting the bases for the two solutions, respectively. The corresponding error in the functional is

$$J[\mathbf{e}] = J[\mathbf{E}^{sc}] - J[\pi_h \mathbf{E}^{sc}], \quad (20)$$

by linearity of  $J$ .

By (16), we can rewrite (20) as

$$\begin{aligned} J[\mathbf{e}] &= \langle \mathbf{e}, \mathbf{p} \rangle \\ &= \langle \mathcal{L}\mathbf{e}, \mathbf{v} \rangle \\ &= \langle \mathbf{R}, \mathbf{v} \rangle, \end{aligned} \quad (21)$$

where  $\mathbf{R} = \mathcal{L}\mathbf{e}$  denotes the residual. Thus, the rationale for referring to (21) as the dual-weighted residual is now self-evident.

By Galerkin orthogonality, the error is orthogonal to the span of  $\pi_h B$ . Hence, we can remove the components of the approximate adjoint solution  $\pi_h \mathbf{v}$  from the “true” adjoint solution  $\mathbf{v}$ . For simplicity, from (12) and (13) we have the symmetric form of  $\langle \mathcal{L}\mathbf{E}^{sc}, \mathbf{v} \rangle$ , where

$$\begin{aligned} \langle \mathcal{L}\mathbf{E}^{sc}, \mathbf{v} \rangle &= \iiint_{\Omega} \mu_r^{-1} \nabla \times \mathbf{E}^{sc} \cdot (\nabla \times \mathbf{v}^*) d\Omega \\ &\quad - \iiint_{\Omega} \mathbf{v}^* \cdot (k_0^2 \varepsilon_r \mathbf{E}^{sc}) d\Omega, \end{aligned} \quad (22)$$

which we denote by  $A(\mathbf{E}^{sc}, \mathbf{v})$ , and therefore

$$\begin{aligned} \langle \mathcal{L}\mathbf{e}, \mathbf{v} \rangle &= \langle \mathbf{R}, \mathbf{v} \rangle \\ &= A(\mathbf{e}, \mathbf{v} - \pi_h \mathbf{v}) \\ &= \langle \mathbf{G}, \mathbf{v} - \pi_h \mathbf{v} \rangle - A(\pi_h \mathbf{E}^{sc}, \mathbf{v} - \pi_h \mathbf{v}). \end{aligned} \quad (23)$$

Generally, in evaluating the error estimate in the form of (23) we do not have access to the “true” solutions for the adjoint problem, so we substitute a higher order approximate solution for  $\mathbf{v}$  and neglect any resultant error in the estimate. Note that utilizing a solution which exists in the same space  $\pi_h B$  renders a useless estimate of zero due to Galerkin orthogonality. Increasing the order of the field expansion by one provides excellent refinement information, though other schemes exist [6].

Note also that the subtraction  $\mathbf{v} - \pi_h \mathbf{v}$  is not explicitly performed, but rather indicates the exclusion of terms shared in the higher order and lower order approximations.

The error term (23) is not evaluated globally, but in a piece-wise fashion, accumulating the appropriate terms per element, or in other schemes, such as per basis function, or per direction. The resulting expressions provide greater versatility for understanding the distribution of local contributions to the error and optimizing the model discretization. For problems with solutions or functionals which depend primarily on a single direction of the electric field in the domain, for example, automatically targeting and improving resolution specifically in those regions minimizes potential inefficiencies, such as unnecessarily increasing the field expansion in less impactful directions, which adds significant computation time for little benefit. Note, it is not possible to leverage such information with a pure local per-element approach to the error estimation.

We have, then, a collection of error contributions for each element  $\tilde{e}_1, \tilde{e}_2, \dots, \tilde{e}_K$ , which sum to the total QoI error estimate  $\tilde{J}$  such that

$$\tilde{J}[\mathbf{e}] = \sum_{i=1}^K \tilde{e}_i, \quad (24)$$

where in general  $\tilde{e}_i \in \mathbb{C}$ , and with which we consider refining either in global-tolerance (GT) schemes or local-tolerance (LT) schemes.

We define GT schemes as those that determine the selection of elements for refinement based on a tolerance on the global error estimate. In this category of refinement, we refine the smallest collection of elements  $c = \{\tilde{e}_l, \dots, \tilde{e}_j\}$  such that

$$\sum_{\tilde{e}_i \in c} |\tilde{e}_i| \geq a \sum_{i=1}^K |\tilde{e}_i|, \quad 0 < a < 1. \quad (25)$$

A fixed  $a$  provides an intrinsically hierarchical refinement process, where finer error tolerances include the iteration procedure of larger tolerances, and therefore the refinement may be inefficient.

Instead, the fraction  $a$  is varied each iteration, with a larger difference between the current error estimate and the desired error tolerance driving larger global refinement.

We therefore provide the following metric:

$$a = 1 - \left( \frac{T}{\sum_{i=1}^K |\tilde{e}_i|} \right)^m, \quad (26)$$

where  $T$  denotes a global error tolerance, and  $m$  controls the aggressiveness of the refinement, with larger values of  $m$  implying more extensive refinement, and correspondingly higher likelihood of over-saturation for a given QoI, though with the potential for reduced number of iterations. We further note that the tolerance  $T$  is not a normalized quantity and therefore an effective choice is dependent on the size of the QoI. We note, however, that even in the absence of prior knowledge about the QoI, the initial discretization (even when very coarse) typically provides an estimate of the QoI within an order of magnitude of the actual value, enabling the automatic selection of  $T$  based on a predefined relative tolerance or desired percent error. If necessary,  $T$  can also be tuned during the refinement procedure as the information available on the magnitude of the QoI improves.

If the global error estimate grossly exceeds that of the tolerance, (26) implies refining the entire discretization. As the global error estimate nears the tolerance, however, the scope of the refinement correspondingly shrinks, helping reduce overshoot and over saturation of the discretization. (26) naturally generalizes to coarsening as well, with a negative value suggesting a reduction in resolution in an analogous manner to that of the refinement.

We also consider refinement based on a LT heuristic that employs an error tolerance on the element contributions of the error to guide the refinement. Assuming ideal conditions in the remainder of analyzing the model (i.e., adequate precision, perfect numerical integration, etc.), the solution and its accuracy wholly depend on the sufficiency of the discretization (the size of the elements, and the field expansion). The *a priori* element contribution is given by

$$|\tilde{e}_i| \approx C h_i^{p_i+1}, \quad (27)$$

where  $C$  is some unknown coefficient,  $h_i$  is the size of the element (e.g., the diameter of the hexahedron), and  $p_i$  denotes

the order of the basis in each element [45]. We desire that the element contribution falls below some threshold  $T$ ,

$$Ch_i^{p_i+1} \leq T. \quad (28)$$

This *a priori* error condition, when combined with the DWR *a posteriori* error estimate permits another approach to refinement.  $C$  is found using (27) with the *a posteriori* error estimate. With each term known, (27) can be manipulated to generate, for instance, an update condition on the element size:

$$h'_i = m \left( \frac{T}{|\bar{\epsilon}_i|} \right)^{\frac{1}{p_i}} h_i, \quad (29)$$

where  $h'_i$  denotes the updated diameter of the  $i^{\text{th}}$  element, and as in the GT refinement heuristic, the quantity  $m$  controls the aggressiveness of the refinement. In such cases where the scaling of  $h_i$  is greater than 1.0, then the estimated resolution is sufficient, and—when possible, either through re-meshing or manipulating the field expansion in the element—can be reduced without violating the desired error tolerance. And, conversely, for scaling of less than 1.0, the resolution ought to be increased.

Analogously to (29), manipulation of (27) can produce an explicit  $p$ -refinement indicator:

$$p'_i = p_i - m(h_i) \log \frac{T}{|\bar{\epsilon}_i|}, \quad (30)$$

where  $p'_i$  denotes the updated field expansion order, and  $m$  tunes the refinement. Specifically, we consider  $m$  as a function of  $h_i$ . Note, most importantly, that both (29) and (30) inherently provide gradation in the refinement or coarsening; this enables efficient “jumps” in the discretization resolution, while also inhibiting overshoots and over-saturation of the model. The overall goal of such refinement is to reach the desired tolerance with a minimal number of steps. Additionally, this approach is conducive to homogenization of error in the discretization, a necessary ingredient for efficient adaptively refined meshes [46], where in the ideal case the error density is constant, as vast differences in error contributions throughout the domain suggest inefficiencies and insufficiencies.

Moreover, summation of the approximate QoI and the error estimate improves accuracy (in many cases substantially), reducing the effective cost of the adjoint solution computation by providing both an automated refinement heuristic and simultaneously improving the accuracy of the QoI itself.

### C. Deriving an Example QoI

For an illustrative example of a QoI, used in the remainder of this paper for numerical results, we study the scattered electric field in the far-field limit corresponding to a direction of interest which we can then apply towards the accurate computation of the monostatic or bistatic RCS.

From the Kirchhoff integral,

$$\mathbf{E}_{FF}^{sc} = \frac{e^{-jk_0 r}}{4\pi r} \oint_S [\hat{\mathbf{n}} \times (\nabla \times \mathbf{E}^{sc}) + jk_0 (\hat{\mathbf{n}} \times \mathbf{E}^{sc} \times \mathbf{i}_r)] e^{jk_0 \mathbf{i}_r \cdot \mathbf{r}'} dS, \quad (31)$$

where  $\hat{\mathbf{n}}$  denotes the surface normal, and  $\mathbf{i}_r$  the scattering direction, we first extract the distance dependent terms by removing the factor  $\frac{e^{-jk_0 r}}{4\pi r}$  from the expression.

Since we require a scalar QoI, we introduce a new vector  $\mathbf{w}$  which isolates a component of the scattered field (e.g., the  $z$ -directed or  $\theta$ -directed component). Hence, we have the following QoI constructed from (31):

$$J[\mathbf{E}^{sc}] = \oint_S \mathbf{w} \cdot [\hat{\mathbf{n}} \times (\nabla \times \mathbf{E}^{sc}) + jk_0 (\hat{\mathbf{n}} \times \mathbf{E}^{sc} \times \mathbf{i}_r)] e^{jk_0 \mathbf{i}_r \cdot \mathbf{r}'} dS. \quad (32)$$

Note, due to the surface-equivalence principle applied in (31), the QoI is computed only from field values on the boundary of the equivalent surface, rather than the fields in the entire volume, which are treated as non-contributing.

## III. NUMERICAL RESULTS

We now demonstrate the utility of the adjoint based *a posteriori* error estimation and adaptive error refinement techniques. Since error estimation and adaptive refinement both benefit naturally from higher-order elements, as  $p$ - and the combined  $hp$ -refinement strategies permit exponential rates of convergence over the algebraic convergence of standard  $h$ -refinement [45], [47]–[49], we demonstrate results using the double higher-order methodology [50]. The model problem is a spherical perfect dielectric scatterer of diameter  $2\lambda$  with relative permittivity  $\epsilon_r = 2.56$  surrounded by a layer of air and with the domain truncated by a layer of PML (both of which have a thickness of  $0.3\lambda$ ) and a PEC boundary, as described in Section III. In the following examples the QoI is the scattered electric field in the direction of the incident plane wave from (32), with  $\mathbf{w}$  matching the polarization of the incident wave.

The formulation of the DWR permits convenient collection of error contributions among different resolutions, as described in Section III. By attaching, for example, an error contribution to each basis function we can construct a QoI error contribution “field” which varies throughout the volume of the model. Fig. 1 illustrates the relative QoI error contribution field for an extremely poor discretization with uniform field expansion. As indicated by the concentric circles, based on this QoI error contribution field plot, the error contribution in the cross-section is largely constrained to the dielectric sphere, with significant emphasis in a conical region in the direction of the far-field QoI.

Now, collecting the error contributions on a per element level instead reveals a similar concentrated distribution of error. With the incident plane wave traveling along the  $x$ -axis and polarized in the  $z$ -direction, the error contributions are distributed symmetrically about this axis, as seen in Fig. 2. Furthermore, the concentration occurs primarily in the region of initial incidence, and decays fairly rapidly outside this region, just as predicted from the QoI error contribution field. This distribution of error contributions, or alternatively, the suggested dependence of the QoI on this region of the discretization provides a perfect candidate for targeted, adaptive refinement, with the ideal result of such refinement being a small overall error and nearly uniform error contribution distribution.

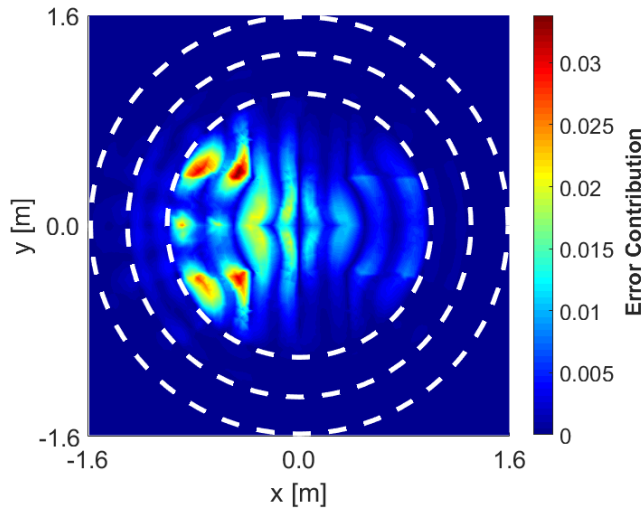


Fig. 1. Planar cut ( $x$ - $y$ ) of the QoI error contribution field magnitude for an extremely coarse uniform discretization with the global QoI error estimate  $\approx 30$ . The concentric circles denote the boundaries of the exterior PML, middle air, and interior dielectric layers.

As derived in Section III, we explore two approaches to conducting refinement based on the information and utility provided by the adjoint solution. To leverage higher-order elements and the improved convergence rates, we investigate application to  $p$ -refinement; with an adequate remeshing routine, the procedure can be repeated identically for  $h$ -refinement, or extended to the combined  $hp$ -refinement.

To fully evaluate the two refinement approaches, in each case the discretizations, consisting of first-order only basis functions and 256 geometrically second-order elements, start with poor initial accuracy. Computing the QoI from this initial discretization to evaluate the RCS produces 40.7% error with respect to the analytical RCS computed from Mie scattering.

We show first the GT refinement heuristic which leverages the DWR estimate to refine a percentage of the total global error estimate as in (26) with  $m = 0.7$ , to provide a balance between rapid refinement and minimizing overshoot. Refinement is repeated until a suitable termination condition is met by increasing the orders of chosen elements by one; in this case we refine until the estimate of the global error falls below a threshold  $T \in \{1.0, 0.7, 0.4, 0.25, 0.15\}$ .

As seen in Fig. 3, which illustrates the DWR estimates of the absolute global error, the GT refinement heuristic requires roughly four iterations per tolerance, excluding the finest tolerance which took five. While not monotonic in the estimated error, the adaptive refinement converges fairly rapidly to the desired tolerance. Note, however, that while not substantial, the level of overshoot is also not insignificant.

According to the GT refinement procedure the field expansion orders are distributed in their final iterations as in Fig. 4.

Lastly, we demonstrate the effectiveness of the LT refinement scheme by combining the *a priori* error estimate with the *a posteriori* estimate to guide the refinement as in (28), and (30) with  $m(h_i) = h_i$ . While the discretizations as above begins with uniformly first order basis functions,

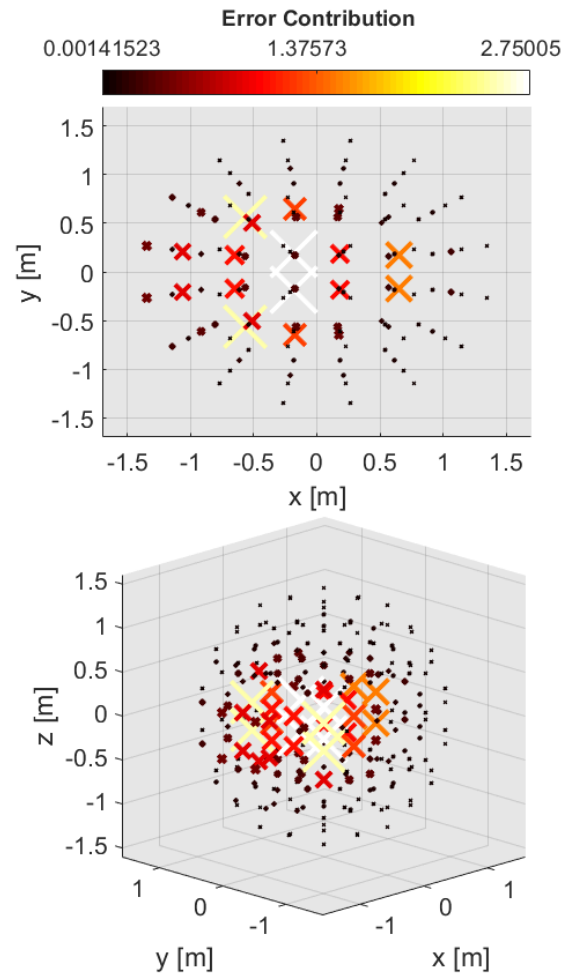


Fig. 2. Spatial distribution of the per element QoI error contribution estimates for the same discretization as in Fig. 1 for 2-D and 3-D perspectives.

this heuristic for refinement simultaneously coarsens when possible and profitable, a potentially significant advantage over other strategies.

Note that in this procedure, we specify a per element error tolerance  $T$  as opposed to a tolerance on the global error, and refinement is conducted such that this tolerance is met as exactly as possible, and in the fewest number of iterations to reduce the computational impact of the intermediate refinement procedure. As a demonstration, we include results for five tolerances: 0.05, 0.03, 0.01, 0.005, 0.003. Each tolerance begins from the same starting discretization from the GT heuristic case. Fig. 5 illustrates the effectiveness of this refinement heuristic. In most cases, only three iterations are required to reach the desired tolerance; in two cases, one additional iteration is needed, but makes only slight adjustments to the distribution of unknowns. This relative independence of the number of iterations required from the desired tolerance implies the efficiency of the underlying refinement method based on the combination of the *a priori* and *a posteriori* error estimates. The first two iterations modify the discretization drastically, closely reaching the desired tolerance, while the third, and potentially fourth iterations incur minor adjustments to reach the desired tolerance without vast overshoots. As such,

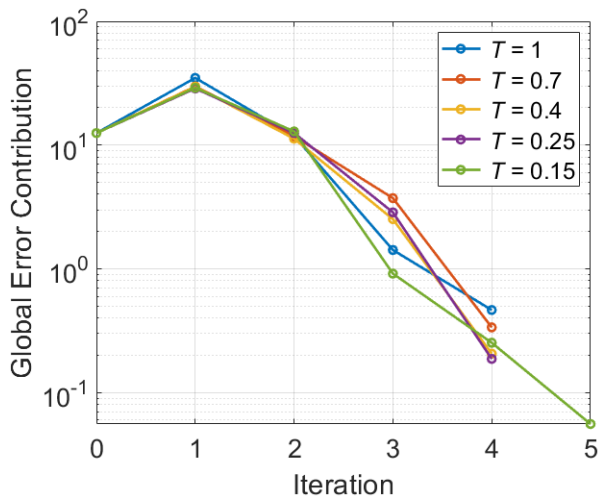


Fig. 3. Global QoI error contribution estimates per iteration for various tolerances with the GT refinement heuristic.

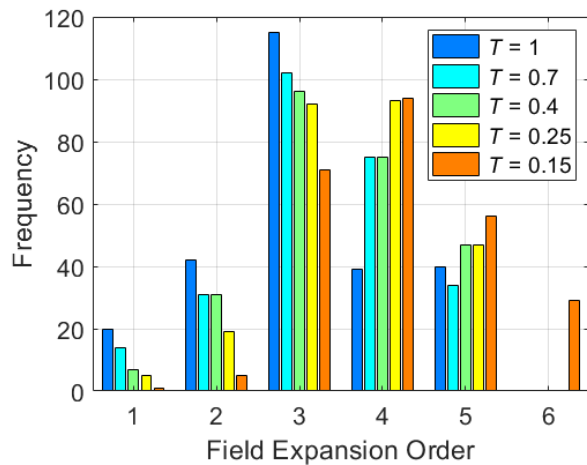


Fig. 4. Final distribution of field expansion orders for various per element error contribution tolerances with the GT refinement heuristic.

when memory constraints permit, it is advisable to store the matrix in the intermediate stages to substantially reduce the computational expense of this refinement heuristic in particular as the final iterations target only a handful of elements.

While not a constraint on the refinement procedure, the DWR expression of the absolute global QoI error at each iteration shows similar behavior, as seen in Fig. 6. Finer per element error contribution tolerances rapidly decrease the overall error contribution estimate.

With these electric field QoI's computed at the desired tolerances, we compare the approximate monostatic RCS to that computed by Mie scattering [52]. The results in Fig. 7, computed for the final iteration of each tolerance in Figs. 5 and 6, show a rapid decrease in the percent error with respect to the analytical solution. Given that the initial accuracy for each tolerance is extremely poor, this further illustrates the effectiveness of the refinement heuristic to tailor the accuracy of the far-field QoI rapidly and without over-saturation.

With the success of the refinement in substantially reducing the discretization error efficiently, revisiting the spatial

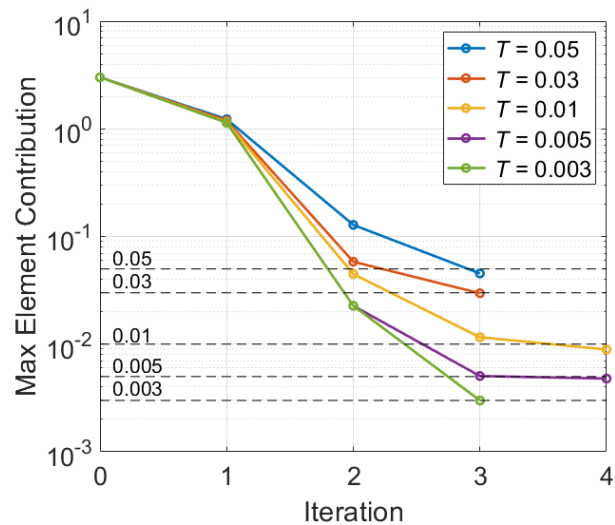


Fig. 5. Maximum per element QoI error contribution estimates per iteration for various tolerances with the LT refinement heuristic.

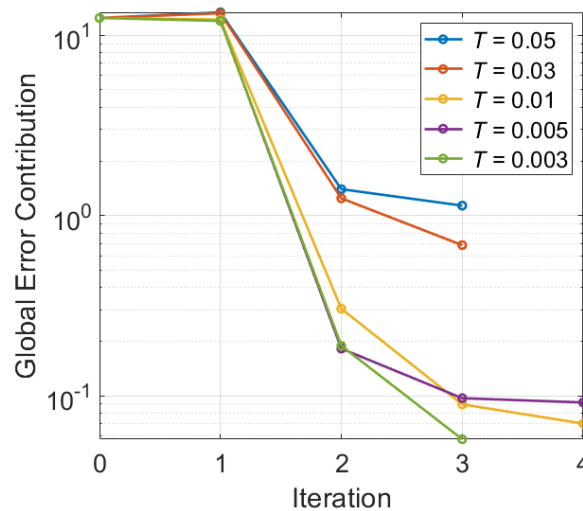


Fig. 6. Global QoI error contribution estimates per iteration for various tolerances with the LT refinement heuristic.

distribution of the QoI error contributions demonstrates the satisfaction of the second goal of homogenizing the error contribution distribution and improving the error density, as seen in Fig. 8. In contrast to the discretization of Fig. 2, as a result of the LT refinement heuristic, the individual QoI error contributions are not only substantially smaller, but the distribution is no longer heavily concentrated, resulting in a substantially improved error density and a more balanced mesh.

Fig. 9 summarizes the distribution of field expansion orders for the tolerances using the LT refinement heuristic. For the finer tolerances, unknowns are automatically introduced where necessary. As expected as well, those finer tolerance attain higher expansion orders at higher rates, while the larger tolerances maintain even first-order basis functions where acceptable for the accuracy of the QoI. Note that in each tolerance, the bulk of the elements cluster around third and fourth field expansion order just as in the GT refinement

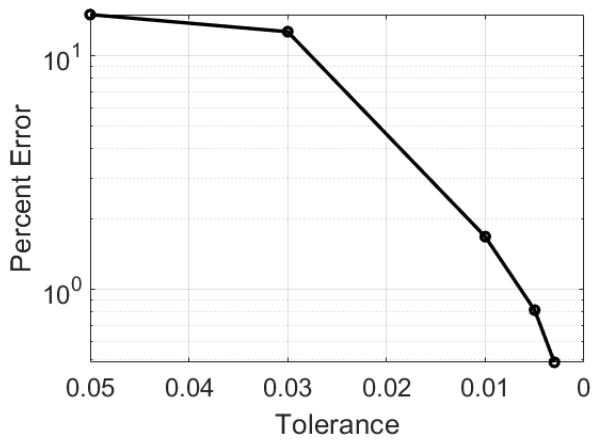


Fig. 7. Percent error with respect to Mie scattering for the monostatic RCS for the final iteration of each tolerance in Fig. 5 with the LT refinement heuristic.

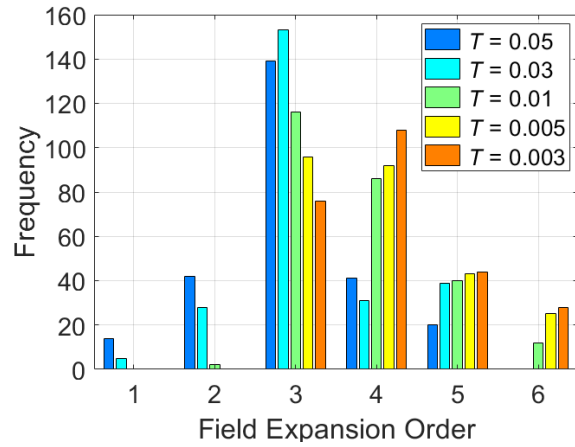


Fig. 9. Final distribution of field expansion orders for various per element error contribution tolerances with the LT refinement heuristic.

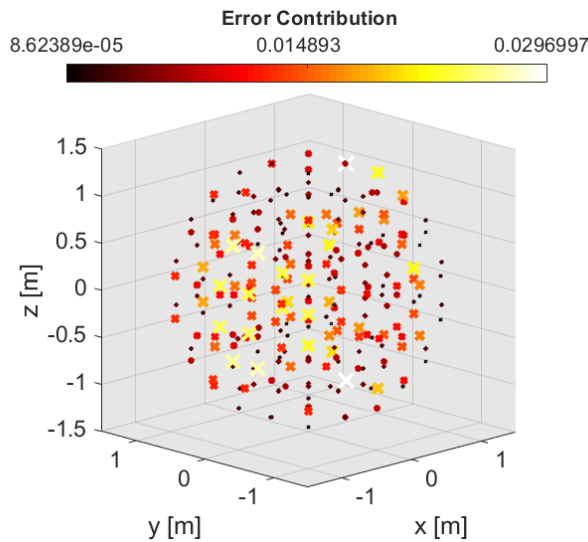


Fig. 8. Spatial distribution of the per element QoI error contribution estimates for the adaptively refined discretization based on the LT heuristic with a tolerance of 0.03.

heuristic.

Comparing the effectiveness of the GT and the LT heuristics, the LT scheme performs moderately better, distributing unknowns more effectively and therefore producing more accurate QoIs for similar cost. The LT heuristic, in addition, satisfies the tolerance almost exactly.

As seen in Fig. 10, for the final discretizations produced by the proposed adaptivity with various levels of tolerance, the LT heuristic exhibits better performance compared to the GT heuristic for finer tolerances and lower percent error with respect to Mie scattering. Specifically, the LT heuristic with the finest tolerance yields an error of 0.49% with 57673 unknowns, while the finest tolerance for the GT heuristic requires 59070 unknowns for an error of 2.36%. For reference, uniform (non-adaptive) refinement is included. To achieve similar accuracy to the LT heuristic, uniform refinement required 36008 additional unknowns. Overall, in these instances the LT heuristic allocates computational resources more effectively, producing higher quality discretizations for fine tolerances,

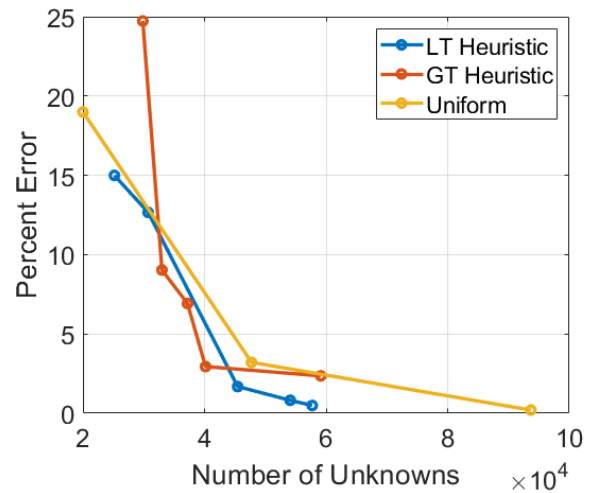


Fig. 10. Convergence of the LT and GT refinement heuristics compared to non-adaptive, uniform refinement.

and in fewer iterations, which saves valuable computation time during the adaptive refinement procedure.

The LT refinement heuristic, then, which leverages both the *a priori* and the *a posteriori* element contributions outperforms the GT heuristic.

#### IV. CONCLUSION

We have demonstrated the effectiveness and utility of adjoint-based methodologies applied to 3-D CEM problems. Providing explicit expressions and derivations of the adjoint problem, along with error contribution estimates and automatic refinement heuristics, this study contains a complete framework to leverage the adjoint solution for highly effective error estimation metrics and fully automated adaptive mesh refinement.

We presented two adaptive mesh refinement heuristics—one based on the global error tolerance, and the other on local error tolerances—which, when coupled with the adjoint solution, intelligently refine the model discretization rapidly and with great accuracy. Even for extremely coarse initial

discretizations, we have demonstrated the capability to automatically produce highly efficient and highly accurate resource allocations specifically tailored to a desired quantity of interest. Although both refinement heuristics perform well, the presented local error tolerance refinement heuristic outperforms the global error tolerance heuristic in number of iterations and accuracy. The local tolerance heuristic is also characterized by relative independence of the desired tolerance from the number of iterations and is therefore suitable and practical for application to automatic refinement to fine tolerances. The results, in addition, indicate vastly improved error density and error homogenization, which further illustrates the efficiency and practicality of the proposed method.

Adjoint-based methodologies, overall, provide significant value and potential to CEM applications, enabling the ability to accurately and efficiently refine models and eliminate discretization error fully automatically. Future works will present the utilization of adjoints for applications in sensitivity analysis, uncertainty quantification, and optimization.

#### ACKNOWLEDGMENT

The authors would like to thank Dr. Michael Gilbert, Program Director, US Air Force Research Laboratory, CREATE SENTRI Program, for his support and guidance on the project and valuable discussions.

#### REFERENCES

- [1] K. Eriksson, D. Estep, P. Hansbo, and C. Johnson, "Introduction to adaptive methods for differential equations," *Acta Numerica*, vol. 4, pp. 105–158, 1995.
- [2] W. Bangerth and R. Rannacher, *Adaptive Finite Element Methods for Differential Equations*. Birkhauser Basel, 2003.
- [3] D. Estep, "A posteriori error bounds and global error control for approximation of ordinary differential equations," *SIAM Journal on Numerical Analysis*, vol. 32, no. 1, pp. 1–48, 1995.
- [4] D. Estep, M. Larson, and W. RD, "Estimating the error of numerical solutions of systems of reaction–diffusion equations," *Memoirs of the American Mathematical Society*, vol. 696, 07 2000.
- [5] D. Estep, M. Holst, and D. Mikulencak, "Accounting for stability: A posteriori error estimates based on residuals and variational analysis," *Communications in Numerical Methods in Engineering*, vol. 18, pp. 15 – 30, 11 2001.
- [6] R. Becker and R. Rannacher, "A feed-back approach to error control in finite element methods: Basic analysis and examples," *East-West J. Numer. Math*, vol. 4, pp. 237–264, 1996.
- [7] G. I. Marchuk, *Adjoint Equations and Analysis of Complex Systems*. Netherlands: Kluwer Academic Publishers, 1995.
- [8] K. Eriksson, D. Estep, P. Hansbo, and C. Johnson, "Introduction to adaptive methods for differential equations," *Acta Numerica*, vol. 4, pp. 105–158, 1995.
- [9] R. Hartmann and P. Houston, "Adaptive discontinuous Galerkin finite element methods for the compressible Euler equations," *Journal of Computational Physics*, vol. 183, no. 2, pp. 508–532, 2002.
- [10] R. Hartmann and P. Houston, "Adaptive discontinuous Galerkin finite element methods for nonlinear hyperbolic conservation laws," *SIAM Journal on Scientific Computing*, vol. 24, no. 3, pp. 979–1004, 2003.
- [11] R. Becker, "Mesh adaptation for stationary flow control," *Journal of Mathematical Fluid Mechanics*, pp. 317–341, 11 2001.
- [12] M. Giles and E. Süli, "Adjoint methods for PDEs: A posteriori error analysis and postprocessing by duality," *Acta Numerica*, vol. 11, pp. 145 – 236, 01 2002.
- [13] M. H. Bakr, *Nonlinear Optimization in Electrical Engineering with Applications in MATLAB*. IET, September 2013.
- [14] M. H. Bakr and N. K. Nikolova, "An adjoint variable method for time domain TLM with fixed structured grids," in *IEEE MTT-S International Microwave Symposium Digest, 2003*, vol. 2, June 2003, pp. 1121–1124 vol.2.
- [15] N. K. Nikolova, H. W. Tam, and M. H. Bakr, "Sensitivity analysis with the FDTD method on structured grids," *IEEE Transactions on Microwave Theory and Techniques*, vol. 52, no. 4, pp. 1207–1216, April 2004.
- [16] S. M. Ali, N. K. Nikolova, and M. H. Bakr, "Central adjoint variable method for sensitivity analysis with structured grid electromagnetic solvers," *IEEE Transactions on Magnetics*, vol. 40, no. 4, pp. 1969–1971, July 2004.
- [17] M. Swillam, M. Bakr, N. Nikolova, and X. Li, "Adjoint sensitivity analysis of dielectric discontinuities using FDTD," *Electromagnetics*, vol. 27, 03 2007.
- [18] M. H. Bakr and N. K. Nikolova, "An adjoint variable method for time-domain transmission-line modeling with fixed structured grids," *IEEE Transactions on Microwave Theory and Techniques*, vol. 52, no. 2, pp. 554–559, Feb 2004.
- [19] M. M. T. Maghrabi, M. H. Bakr, and S. Kumar, "Linear adjoint sensitivity analysis of the time-dependent schrödinger equation," in *2019 International Applied Computational Electromagnetics Society Symposium (ACES)*, April 2019, pp. 1–2.
- [20] P. Garcia and J. P. Webb, "Optimization of planar devices by the finite element method," *IEEE Transactions on Microwave Theory and Techniques*, vol. 38, no. 1, pp. 48–53, Jan 1990.
- [21] S. Koziel and A. Bekasiewicz, "Fast EM-driven size reduction of antenna structures by means of adjoint sensitivities and trust regions," *IEEE Antennas and Wireless Propagation Letters*, vol. 14, pp. 1681–1684, 2015.
- [22] M. M. Botha and D. B. Davidson, "The implicit, element residual method for a posteriori error estimation in FE-BI analysis," *IEEE Transactions on Antennas and Propagation*, vol. 54, no. 1, pp. 255–258, Jan 2006.
- [23] M. M. Botha and D. B. Davidson, "An explicit a posteriori error indicator for electromagnetic, finite element-boundary integral analysis," *IEEE Transactions on Antennas and Propagation*, vol. 53, no. 11, pp. 3717–3725, Nov 2005.
- [24] S. M. Schnepf, "Error-driven dynamical hp-meshes with the discontinuous Galerkin method for three-dimensional wave propagation problems," *Journal of Computational and Applied Mathematics*, vol. 270, pp. 353 – 368, 2014.
- [25] P. Monk and E. Süli, "The adaptive computation of far-field patterns by a posteriori error estimation of linear functionals," *SIAM Journal on Numerical Analysis*, vol. 36, no. 1, pp. 251–274, 1998.
- [26] P. Monk, "A posteriori error indicators for Maxwell's equations," *Journal of Computational and Applied Mathematics*, vol. 100, no. 2, pp. 173 – 190, 1998.
- [27] P. Ingelstrom and A. Bondeson, "Goal-oriented error estimation and h-adaptivity for Maxwell's equations," *Computer Methods in Applied Mechanics and Engineering*, vol. 192, pp. 2597–2616, 06 2003.
- [28] P. Ingelstrom and A. Bondeson, "Goal-oriented error-estimation for S-parameter computations," *IEEE Transactions on Magnetics*, vol. 40, no. 2, pp. 1432–1435, 2004.
- [29] J. P. Webb, "Using adjoint solutions to estimate errors in global quantities," *IEEE Transactions on Magnetics*, vol. 41, no. 5, pp. 1728–1731, 2005.
- [30] L. Demkowicz, "Fully automatic hp-adaptivity for Maxwell's equations," *Computer Methods in Applied Mechanics and Engineering*, vol. 194, no. 2, pp. 605 – 624, 2005.
- [31] L. Demkowicz, *Computing with hp Finite Elements I. One- and Two-Dimensional Elliptic and Maxwell Problems*. Chapman & Hall/CRC Press, Taylor and Francis, 2007.
- [32] L. E. García-Castillo, D. Pardo, I. Gómez-Revuelto, and L. F. Demkowicz, "A two-dimensional self-adaptive hp finite element method for the characterization of waveguide discontinuities. Part I: Energy-norm based automatic hp-adaptivity," *Computer Methods in Applied Mechanics and Engineering*, vol. 196, no. 49, pp. 4823 – 4852, 2007.
- [33] I. Gomez-Revuelto, L. E. Garcia-Castillo, S. Llorente-Romano, and D. Pardo, "A three-dimensional self-adaptive hp finite element method for the characterization of waveguide discontinuities," *Computer Methods in Applied Mechanics and Engineering*, vol. 249–252, pp. 62 – 74, 2012.
- [34] D. Pardo, L. E. García-Castillo, L. F. Demkowicz, and C. Torres-Verdín, "A two-dimensional self-adaptive hp finite element method for the characterization of waveguide discontinuities. Part II: Goal-oriented hp-adaptivity," *Computer Methods in Applied Mechanics and Engineering*, vol. 196, no. 49, pp. 4811 – 4822, 2007.
- [35] L. E. Garcia-Castillo, D. Pardo, and L. F. Demkowicz, "Energy-norm-based and goal-oriented automatic hp adaptivity for electromagnetics:

- Application to waveguide discontinuities," *IEEE Transactions on Microwave Theory and Techniques*, vol. 56, no. 12, pp. 3039–3049, 2008.
- [36] I. Gomez-Revenuto, L. Garcia-Castillo, and M. Palma, "Goal-oriented self-adaptive  $hp$ -strategies for finite element analysis of electromagnetic scattering and radiation problems," *Progress In Electromagnetics Research*, vol. 125, pp. 459–482, 01 2012.
- [37] D. Pardo, L. Demkowicz, C. Torres-Verdin, and M. Paszynski, "A self-adaptive goal-oriented  $hp$ -finite element method with electromagnetic applications. Part II: Electrodynamics," *Computer Methods in Applied Mechanics and Engineering*, vol. 196, no. 37, pp. 3585 – 3597, 2007.
- [38] A. Zdunek and W. Rachowicz, "A goal-oriented  $hp$ -adaptive finite element approach to radar scattering problems," *Computer Methods in Applied Mechanics and Engineering*, vol. 194, no. 2, pp. 657 – 674, 2005.
- [39] C. Key, A. P. Smull, D. Estep, T. Butler, and B. M. Notaroš, "A posteriori error estimation and adaptive discretization refinement using adjoint methods in CEM: A study with a 1-D higher order FEM scattering example," *IEEE Transactions on Antennas and Propagation*, vol. 68, no. 5, pp. 3791–3806, 2020.
- [40] J. Harmon and B. M. Notaroš, "The dual weighted residual and error estimation in double higher-order FEM," in *2019 IEEE International Symposium on Antennas and Propagation and USNC-URSI Radio Science Meeting*, July 2019, pp. 771–772.
- [41] J. Harmon, C. Key, B. M. Notaroš, D. Estep, and T. Butler, "Adjoint-based uncertainty quantification in frequency-domain double higher-order FEM," in *2019 International Applied Computational Electromagnetics Society Symposium (ACES)*, April 2019, pp. 1–2.
- [42] B. M. Notaroš, J. Harmon, C. Key, D. Estep, and T. Butler, "Error estimation and uncertainty quantification based on adjoint methods in computational electromagnetics," in *2019 IEEE International Symposium on Antennas and Propagation and USNC-URSI Radio Science Meeting*, July 2019, pp. 221–222.
- [43] B. M. Notaroš, S. B. Manić, C. Key, J. Harmon, and D. Estep, "Overview of some advances in higher order frequency-domain CEM techniques," in *2019 International Conference on Electromagnetics in Advanced Applications (ICEAA)*, Sep. 2019, pp. 1330–1333.
- [44] A. P. Smull, A. B. Manić, S. B. Manić, and B. M. Notaroš, "Anisotropic locally conformal perfectly matched layer for higher order curvilinear finite-element modeling," *IEEE Transactions on Antennas and Propagation*, vol. 65, no. 12, pp. 7157–7165, Dec 2017.
- [45] I. Babuška and M. Suri, "The  $p$  and  $h$ - $p$  versions of the finite element method, basic principles and properties," *SIAM Review*, vol. 36, no. 4, pp. 578–632, 1994.
- [46] K. Chen, "Error equidistribution and mesh adaptation," *SIAM Journal on Scientific Computing*, vol. 15, no. 4, pp. 798–818, 1994.
- [47] W. Gui and I. Babuška, "The  $h$ ,  $p$  and  $h$ - $p$  versions of the finite element method in 1 dimension: Part III," *Numerische Mathematik*, vol. 49, no. 6, pp. 659–683, Nov 1986.
- [48] W. Gui and I. Babuška, "The  $h$ ,  $p$  and  $h$ - $p$  versions of the finite element method in 1 dimension: Part II," *Numerische Mathematik*, vol. 49, no. 6, pp. 613–657, Nov 1986.
- [49] I. Babuška and A. Miller, "The post-processing approach in the finite element method—part 3: A posteriori error estimates and adaptive mesh selection," *International Journal for Numerical Methods in Engineering*, vol. 20, no. 12, pp. 2311–2324, 1984.
- [50] M. M. Ilic and B. M. Notaroš, "Higher order large-domain hierarchical FEM technique for electromagnetic modeling using Legendre basis functions on generalized hexahedra," *Electromagnetics*, vol. 26, pp. 517–529, 10 2006.
- [51] P. D. Lax, *Functional Analysis*. New York, NY, USA: Wiley, 2002.
- [52] J.-M. Jin, *Theory and Computation of Electromagnetic Fields*. Hoboken, NJ, USA: Wiley, 2015.



**Jake J. Harmon** (S'19) was born in Fort Collins, CO in 1996. He received his B.S. (*summa cum laude*) in 2019 and is currently pursuing his Ph.D. in Electrical Engineering from Colorado State University. His current research interests include adaptive numerical methods, uncertainty quantification, computational geometry, and higher order modeling in the finite element method and surface integral equation method of moments.



**Cam Key** (S'16) was born in Fort Collins, CO in 1996. He received his B.S. (2018) and is currently pursuing his Ph.D. in Electrical and Computer Engineering from Colorado State University. His current research interests include uncertainty quantification, error prediction, and optimization for computational science and engineering; computational geometry, meshing, data science, machine learning, artificial intelligence, remote sensing and GIS, and novel applications of numerical methods across disciplines



**Donald Estep** received his B.A. in Mathematics from Columbia University in 1981 and his M.S. and Ph.D. in Applied Mathematics from the University of Michigan in 1987.

From 1987–2002, he was a faculty member in the School of Mathematics at the Georgia Institute of Technology. He joined the Department of Mathematics at Colorado State University in 2000 and moved to the Department of Statistics in 2006, serving as Chair from 2017–2019. In 2019, he moved to the Department of Statistics and Actuarial Science at

Simon Fraser University to assume the position of Director of the Canadian Statistical Sciences Institute.

Dr. Estep was appointed University Interdisciplinary Research Scholar in 2009 and University Distinguished Professor in 2017 at Colorado State University. He served as Co-Organizer and first Chair of the SIAM Activity Group on Uncertainty Quantification from 2010–12, and Co-Editor in Chief (founding) of the SIAM/ASA Journal on Uncertainty Quantification from 2012–2017. He won the Computational and Mathematical Methods in Science and Engineering Prize in 2005, held the Chalmers Jubilee Professorship at Chalmers University of Technology from 2013–2014, and was appointed Fellow of the Society for Industrial and Applied Mathematics in 2014.



**Troy Butler** received his B.S. in electrical engineering (2003) followed by his M.S. (2005) and Ph.D. (2009) in mathematics from Colorado State University.

From 2009–12, Dr. Butler was a Postdoctoral Research Fellow (2009–11) and Research Associate (2011–12) in the Computational Hydraulics Group housed within the Institute for Computational Engineering and Sciences at The University of Texas at Austin. From 2012–13, Dr. Butler was a Research Scientist in the Department of Statistics at Colorado

State University. In Fall 2013, Dr. Butler joined CU Denver as an Assistant Professor in Mathematical and Statistical Sciences and was promoted with tenure to Associate Professor in 2019. From 2014–17, Dr. Butler served as the Director for the Center for Computational Mathematics at CU Denver.



**Branislav M. Notaroš** (M'00–SM'03–F'16) received the Dipl.Ing. (B.S.), M.S., and Ph.D. degrees in electrical engineering from the University of Belgrade, Belgrade, Yugoslavia, in 1988, 1992, and 1995, respectively.

From 1996 to 1999, he was Assistant Professor in the School of Electrical Engineering at the University of Belgrade. He was Assistant and Associate Professor from 1999 to 2006 in the Department of Electrical and Computer Engineering at the University of Massachusetts Dartmouth. He is currently

Professor of Electrical and Computer Engineering, University Distinguished Teaching Scholar, and Director of Electromagnetics Laboratory at Colorado State University.

Dr. Notaroš serves as General Chair of the 2022 IEEE International Symposium on Antennas and Propagation and USNC-URSI National Radio Science Meeting and is Associate Editor for the IEEE Transactions on Antennas and Propagation. He serves as Vice President of Applied Computational Electromagnetics Society (ACES) and as Vice-Chair of USNC-URSI Commission B. He was the recipient of the 2005 IEEE MTT-S Microwave Prize, 1999 IEE Marconi Premium, 2019 ACES Technical Achievement Award, 2015 ASEE ECE Distinguished Educator Award, 2015 IEEE Undergraduate Teaching Award, and many other research and teaching international and national awards.